

Cornell potential in generalized Soft Wall holographic model

Sergey Afonin* and Timofey Solomko

Saint Petersburg State University, 7/9 Universitetskaya nab., St.Petersburg, 199034, Russia

Abstract

We derive and analyze the confinement potential of the Cornell type within the framework of the generalized Soft Wall holographic model that includes a parameter controlling the intercept of the linear Regge spectrum. In the phenomenology of Regge trajectories, this parameter is very important for the quantitative description of experimental data. Our analysis shows that the “linear plus Coulomb” confinement potential obtained in the scalar channel is *quantitatively* consistent with the phenomenology and lattice simulations while the agreement in the vector channel is qualitative only. This result indicates the key role of the vacuum scalar sector in the formation of the confinement potential. As a by-product the overall consistency of our holographic description of confinement potential seems to confirm the glueball nature of the scalar meson $f_0(1500)$.

1 Introduction

The quark confinement remains an unresolved key problem of strong interactions despite a tremendous number of works devoted to this subject. One of the basic observables relevant to confinement is the heavy-quark potential. In the real life, this potential is saturated at a constant level at large enough (of the order of 1 fm) distances because of the light quark-antiquark pairs popping up out of the vacuum and thereby completely screening the static sources. But the approximation of heavy static quarks allows to simplify the problem and to address it both analytically within various phenomenological models and in lattice simulations directly from QCD. For this reason, the limit of heavy static quarks is interesting and informative.

The detailed lattice simulations of the form of the heavy-quark potential (see, e.g., the review [1]) revealed a remarkable agreement with the Cornell potential [2],

$$V(r) = -\frac{\kappa}{r} + \sigma r + \text{const.} \quad (1.1)$$

This result imposes a serious restriction on viable phenomenological approaches to strong interactions: In the non-relativistic limit, they should be able to reproduce the behavior (1.1).

One of such promising approaches that passes the given test is the so-called Soft-Wall (SW) holographic model [3, 4]. This popular bottom-up AdS/QCD approach was originally inspired by the AdS/CFT correspondence in string theory [5–7] and turned out to be unexpectedly successful in the description of hadron Regge spectroscopy, hadron form-factors, QCD thermodynamics, and other phenomenology related to the non-perturbative strong interactions (many contemporary references are collected in Ref. [8]). The heavy-quark potential was first calculated within the

*E-mail: s.afonin@spbu.ru.

SW holographic model by Andreev and Zakharov in Ref. [9] and their result agreed with (1.1). The analysis in Ref. [9], however, was performed only for one particular case of the SW model: The vector model with a fixed (simplest) intercept of string like mass spectrum, $m_n^2 = an$, where $n = 1, 2, \dots$. In view of high citation of this analysis in the literature, it is interesting to extend it to arbitrary intercept of linear radial Regge spectrum, $m_n^2 = a(n+b)$, and to the case of scalar SW model. To the best of our knowledge, such extensions were not considered in the literature. The purpose of our present work is to fill this gap. Since the intercept b parametrizes important effects of low-energy strong interactions and is indispensable for making quantitative phenomenological predictions, the holographic derivation and analysis of heavy-quark potential in the presence of nontrivial intercept should provide an interesting test for overall phenomenological consistency of the approach.

The linear confinement potential was also recovered in a closely related AdS/QCD approach called the light-front holographic QCD [10] and a good numerical agreement was observed, see Refs. [11, 12] for the corresponding discussions. A similar conclusion will be made in our work: We will demonstrate that the generalized SW holographic model leads to a good quantitative description of the shape of the Cornell potential (1.1).

The paper is organized as follows. In Section 2, the general design of generalized SW holographic model is presented. The derivation of potential energy between static sources from Holographic Wilson loop within the generalized vector SW model is given in Section 3. The large and small distance asymptotics of this energy are calculated in Sections 4 and 5, respectively. Some technical details are transferred to the Appendices. In Section 6, we extend the results to the generalized scalar SW holographic model. The phenomenological predictions are discussed in Section 7. We conclude in Section 8.

2 Generalized Soft Wall holographic model

The standard SW holographic model is defined by the 5D action [3]

$$S = \int d^4x dz \sqrt{g} e^{-cz^2} \mathcal{L}, \quad (2.1)$$

where $g = |\det g_{MN}|$, \mathcal{L} is a Lagrangian density of some free fields in AdS₅ space which, by assumption, are dual on the AdS₅ boundary to some QCD operators. The metric is given by the Poincaré patch of the AdS₅ space,

$$g_{MN} dx^M dx^N = \frac{R^2}{z^2} (\eta_{\mu\nu} dx^\mu dx^\nu - dz^2), \quad z > 0. \quad (2.2)$$

Here $\eta_{\mu\nu} = \text{diag}(1, -1, -1, -1)$, R denotes the radius of AdS₅ space, and z is the holographic coordinate which has the standard physical interpretation of the inverse energy scale. The static dilaton background e^{-cz^2} (with $c > 0$ in the original model of Ref. [3]) gives rise to Regge behavior of mass spectrum. The standard SW model is defined in the probe approximation, i.e., the metric is not backreacted by matter fields and dilaton — such backreaction is assumed to be suppressed in the large- N_c limit (it should be recalled that, strictly speaking, the holographic approach is formulated in this limit only). There are many bottom-up holographic models based on Einstein-dilaton gravity that provide backgrounds consistent with Einstein equations. This line of research was pioneered in the work [13], the most recent review is presented in [14]. The great advantage of the probe approximation is its simplicity which allows analytical control at each stage. In

relation to our task, extracting the confinement potential beyond this approximation would be a hard technical problem. On the other hand, we will argue that our approach leads (effectively) to a certain phenomenological model for spin-dependent backreaction to the AdS metric by an injected particle.

The Lagrangian density of the simplest SW model describing vector mesons is [3]

$$\mathcal{L} = -\frac{1}{4}F_{MN}F^{MN} + \frac{1}{2}m_5^2 V_M V^M, \quad (2.3)$$

where $F_{MN} = \partial_M V_N - \partial_N V_M$, $M, N = 0, 1, 2, 3, 4$. According to the standard prescriptions of AdS/CFT correspondence [6, 7], the 5D mass m_5 is determined by the behavior of p -form fields near the UV boundary $z = 0$,

$$m_5^2 R^2 = (\Delta - p)(\Delta + p - 4), \quad (2.4)$$

where Δ denotes the scaling dimension of 4D operator dual to the corresponding 5D field on the UV boundary. In the vector case $p = 1$, thus $m_5^2 R^2 = (\Delta - 1)(\Delta - 3)$. The canonical dimension of vector current operator in QCD is $\Delta = 3$ that leads to $m_5 = 0$. This corresponds to massless 5D vector fields which are usually considered in the SW models.

The 4D mass spectrum of the model can be found, as usual, from the equation of motion accepting the 4D plane-wave ansatz $V_\mu(x, z) = e^{ipx} v(z) \epsilon_\mu$ with the on-shell, $p^2 = m^2$, and transversality, $p^\mu \epsilon_\mu = 0$, conditions. Here, $v(z)$ is a profile function for physical 4D modes. In addition, the condition $V_z = 0$ is implied for the physical components of 5D fields [10]. For massless vector fields, this is equivalent to the standard choice of axial gauge due to emerging gauge invariance [3]. The equation of motion ensuing from the action (2.3) for $m_5 = 0$ is

$$\partial_z \left(\frac{e^{-cz^2}}{z} \partial_z v_n \right) = -\frac{m_n^2}{z} e^{-cz^2} v_n, \quad (2.5)$$

The particle-like excitations correspond to normalizable solutions of Sturm-Liouville equation (2.5), which are enumerated by the index n . It is convenient to make the substitution

$$v_n = z^{1/2} e^{cz^2/2} \psi_n, \quad (2.6)$$

that transforms the Eq. (2.5) into a form of one-dimensional Schrödinger equation

$$-\partial_z^2 \psi_n + V(z) \psi_n = m_n^2 \psi_n, \quad (2.7)$$

with the potential

$$V(z) = c^2 z^2 + \frac{3}{4z^2}. \quad (2.8)$$

The mass spectrum of the model is given by the eigenvalues of Eq. (2.7),

$$m_n^2 = 4|c|n, \quad n = 1, 2, \dots \quad (2.9)$$

There exists another formulation of SW model proposed independently and almost simultaneously in Ref. [4], in which the dilaton background is absent but the AdS₅ metric is modified,

$$g_{MN} = \text{diag} \left\{ \frac{R^2}{z^2} h, \dots, \frac{R^2}{z^2} h \right\}, \quad h = e^{-2cz^2}. \quad (2.10)$$

The resulting equation of motion and spectrum are the same. Other formulations of SW holographic model are also possible. They are analyzed in detail in the recent work [8].

The generalized SW holographic model describes the linear spectrum with arbitrary intercept regulated by a parameter b . In the vector case, the generalization of spectrum (2.9) is

$$m_n^2 = 4|c|(n + b), \quad n = 1, 2, \dots \quad (2.11)$$

As was shown in [15] and further developed in [8], the spectrum (2.11) arises in the following generalization of the action of vector SW model,

$$S = \int d^4x dz \sqrt{g} e^{-cz^2} U^2(b, 0, |cz^2|) \mathcal{L}, \quad (2.12)$$

where U is the Tricomi hypergeometric function that modifies the dilaton background. It should be remarked that any other modification of quadratic dilaton background, either manually or by considering a backreacted geometry, will lead to a distortion of the exact Regge behavior, $m_n^2 \sim n$, for any n [8] (and can even lead to a finite number of excitations [16]).

The generalized SW model can be also reformulated in the form of the modified metric (2.10). Generically, if a 5D holographic model describing spin- J mesons contains a z -dependent background $B(z)$ in its action,

$$S = \int d^4x dz \sqrt{g} B(z) \mathcal{L}, \quad (2.13)$$

this action can be rewritten in the form

$$S = \int d^4x dz \sqrt{\tilde{g}} \tilde{\mathcal{L}}, \quad (2.14)$$

with the modified metric [8]

$$\tilde{g}_{MN} = B^{(3/2-J)^{-1}} g_{MN}. \quad (2.15)$$

Substituting the background $B(z)$ in the action (2.12) for spin $J = 1$, we obtain the following generalization for the function h in the modified metric (2.10),

$$h = e^{-2cz^2} U^4(b, 0, |cz^2|). \quad (2.16)$$

This modification will be the starting point for our further analysis of Cornell potential within the generalized SW holographic model.

A question may appear how should we interpret the result (2.15) which would imply that there could be different 5D metrics for fields of different spin? On the one hand, this is a formal consequence of rewriting of the action (2.13) in the form of the action (2.14). The first action is for fields which describe particles of arbitrary integer spin moving in the AdS space with universal z -dependent dilaton background. The second action describes particles moving in a modified AdS space without background but the modification of AdS metric becomes spin-dependent. The modification of metric is such that the harmonic oscillatory part of the potential (2.8) in the equation of motion remains universal for any spin and this provides the universal slope for Regge trajectories (which is an important manifestation of confinement). On the other hand, the second formulation of generalized SW model becomes primary for analysis of confinement properties, thus there should be some physics behind such a mathematical reformulation. We may give the following qualitative physical meaning to the second description. In a space with confining geometry, particle moves around the minimum of its effective gravitational potential

energy [10]. But part of this effective gravitational potential can arise dynamically due to the backreaction of the particle mass (that depends on the particle spin) to the geometry of the environment. The relation (2.15) can be then interpreted as a phenomenological model for this backreaction.

Concluding the reminder we would make the following remark. The linear Regge like spectrum is usually interpreted as a manifestation of confinement. Within the Light-Front holographic QCD [10], the holographic coordinate z has the physical meaning of the measure of the distance between a quark and an antiquark. Then z is proportional to r in the Cornell potential (1.1). In this case, the holographic potential (2.8) can be interpreted, up to an additive constant, as the square of the real potential energy (1.1) between static quarks. The form of Cornell potential (1.1) is then hinted in (2.8). On the heuristic level, if the energy E in the Schrödinger equation is replaced by the energy squared E^2 (as is suggested by the Lorentz invariance in the static limit), then the oscillator potential leads to the behavior $E^2 \sim r^2$ at large distance r , i.e., to the linearly rising potential energy $E \sim r$. In a sense, it is this situation that is encoded in the SW holographic model. For the case of Light-Front holographic QCD, this point is discussed in detail in Ref. [12].

3 Holographic Wilson loop

The analytic and lattice calculations of the potential between static sources are usually based on the analysis of a Wilson loop. The holographic variant of this analysis was developed by Maldacena in Ref. [17]. Within the holographic framework, one considers a Wilson loop \mathcal{L} placed in the 4D boundary of the 5D space with the time coordinate ranging from 0 to T and the remaining 3D spatial coordinates y from $-r/2$ to $r/2$, see Figure 1. The expectation value of the loop in the limit of $T \rightarrow \infty$ is as usual

$$\langle W(\mathcal{C}) \rangle \sim e^{-TE(r)}, \quad (3.1)$$

where $E(r)$ is the energy of the quark-antiquark pair. Alternatively, this expectation value can be obtained via

$$\langle W(\mathcal{C}) \rangle \sim e^{-S}, \quad (3.2)$$

where S represents the area of a string world-sheet which produces the loop \mathcal{L} . Combining these two equations one can compute the energy (the static potential) of configuration as

$$E = \frac{S}{T}. \quad (3.3)$$

The natural choice for the world-sheet area is the Nambu-Goto action

$$S = \frac{1}{2\pi\alpha'} \int d^2\xi \sqrt{\det g_{MN} \partial_\alpha X^M \partial_\beta X^N}, \quad (3.4)$$

where α' is the inverse string tension, X^M are the string coordinates functions which provide a mapping from the (ξ_1, ξ_2) parameter space of the world-sheet into the spacetime, and g_{MN} is the modified Euclidean AdS metric

$$g_{MN} = \text{diag} \left\{ \frac{R^2}{z^2} h, \dots, \frac{R^2}{z^2} h \right\}. \quad (3.5)$$

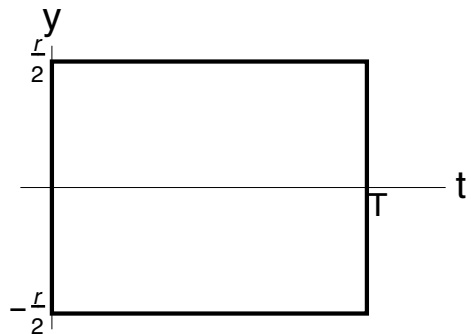


Figure 1: A Wilson loop.

The background function $h(z)$ specifies a holographic model, the general requirement is that the metric must be asymptotically AdS at $z \rightarrow 0$. After choosing $\xi_1 = t$ and $\xi_2 = y$ as the parametrization of the world-sheet and integration over t from 0 to T , the action can be rewritten as

$$S = \frac{TR^2}{2\pi\alpha'} \int_{-r/2}^{r/2} dy \frac{h}{z^2} \sqrt{1+z'^2}, \quad (3.6)$$

where $z' = dz/dy$. From the first integral of this action, which corresponds to the action's translational invariance, one can then obtain an integral expression for the distance r , the end result is

$$r = 2\sqrt{\frac{\lambda}{c}} \int_0^1 dv \frac{h_0}{h} \frac{v^2}{\sqrt{1-v^4 \frac{h_0^2}{h^2}}}, \quad (3.7)$$

where we introduced a new notation,

$$z_0 \equiv z|_{y=0}, \quad h_0 \equiv h|_{z=z_0}, \quad v \equiv \frac{z}{z_0}, \quad \lambda \equiv cz_0^2. \quad (3.8)$$

The expression for the energy is obtained from the equation (3.3) and the action (3.6) by replacing the integration over y with the integration over v by using (3.7) (note that r is equal to the integral over dy from $-r/2$ to $r/2$). The end result is

$$E = \frac{R^2}{\pi\alpha'} \sqrt{\frac{c}{\lambda}} \int_0^1 \frac{dv}{v^2} \frac{h}{\sqrt{1-v^4 \frac{h_0^2}{h^2}}}. \quad (3.9)$$

The details of these derivations can be found, e.g., in Ref. [18].

This integral in (3.9) is evidently divergent at $v = 0$ due to the v^2 in the denominator of the integrand. To solve this problem we introduce a regularization by imposing a cutoff $\varepsilon \rightarrow 0$

$$E = \frac{R^2}{\pi\alpha'} \sqrt{\frac{c}{\lambda}} \int_0^1 \frac{dv}{v^2} \left(\frac{h(\lambda, v)}{\sqrt{1-v^4 \frac{h_0^2}{h^2}}} - D \right) + \frac{R^2}{\pi\alpha'} \sqrt{\frac{c}{\lambda}} D \int_{\varepsilon/z_0}^1 \frac{dv}{v^2}, \quad (3.10)$$

where the regularization constant is defined as

$$D \equiv h|_{v=0}. \quad (3.11)$$

The second integral can be easily computed (here, we temporarily switch notation back to $1/z_0 = \sqrt{c/\lambda}$)

$$\frac{R^2}{\pi\alpha'} \frac{D}{z_0} \int_{\varepsilon/z_0}^1 \frac{dv}{v^2} = -\frac{R^2}{\pi\alpha'} \frac{D}{z_0} \frac{1}{v} \Big|_{\varepsilon/z_0}^1 = \frac{R^2}{\pi\alpha'} \frac{D}{z_0} \left(\frac{z_0}{\varepsilon} - 1 \right) = \frac{R^2 D}{\pi\alpha' \varepsilon} - \frac{R^2 D}{\pi\alpha' z_0}. \quad (3.12)$$

Then we introduce the *regularized energy*

$$E_R = \frac{R^2 D}{\pi\alpha' \varepsilon} + E, \quad (3.13)$$

with the corresponding redefinition of the energy itself as

$$E = \frac{R^2}{\pi\alpha'} \sqrt{\frac{c}{\lambda}} \left[\int_0^1 \frac{dv}{v^2} \left(\frac{h}{\sqrt{1 - v^4 \frac{h_0^2}{h^2}}} - D \right) - D \right]. \quad (3.14)$$

Consider now the case of generalized vector SW holographic model. According to the discussions in Section 2, the background function is given by the expression (2.16). The background used by Andreev and Zakharov in Ref. [9] had the opposite sign in the exponent to enforce a confining geometry. We will use the result (2.16) to generalize the Andreev-Zakharov deformed AdS metric, i.e., we will investigate the confinement properties of SW model with the following generalized background function ($c > 0$),

$$h = e^{2cz^2} U^4(b, 0, cz^2) = e^{2\lambda v^2} U^4(b, 0, \lambda v^2). \quad (3.15)$$

Substituting (3.15) into the integrals for the distance (3.7) and the energy (3.14) we get

$$r = 2\sqrt{\frac{\lambda}{c}} \int_0^1 dv \frac{U^4(b, 0, \lambda)}{U^4(b, 0, \lambda v^2)} \frac{v^2 e^{2\lambda(1-v^2)}}{\sqrt{1 - v^4 e^{4\lambda(1-v^2)} \frac{U^8(b, 0, \lambda)}{U^8(b, 0, \lambda v^2)}}}, \quad (3.16)$$

$$E = \frac{R^2}{\pi\alpha'} \sqrt{\frac{c}{\lambda}} \left[\int_0^1 \frac{dv}{v^2} \left(\frac{e^{2\lambda v^2} U^4(b, 0, \lambda v^2)}{\sqrt{1 - v^4 e^{4\lambda(1-v^2)} \frac{U^8(b, 0, \lambda)}{U^8(b, 0, \lambda v^2)}}} - D \right) - D \right], \quad (3.17)$$

where the regularization constant is $D = U^4(b, 0, 0)$.

The last two expressions determine the energy as a function of the distance in the parametric form. Our next goal is to obtain small and large distance behavior of the energy. In order to derive the corresponding $E(r)$ asymptotics we have to map them into corresponding λ asymptotics of r and E . We will first focus on the large distance asymptotics.

4 Large distance potential

Since the potential $E(r)$ is defined in a parametric form, one has to establish a correspondence between large distances and the range of values of the parameter λ via the analysis of the integrals (3.16) and (3.17). Note that these integrals must be real-valued, and as such the expression under the square root must be greater than zero within the integration range, $v \in [0, 1]$,

$$1 - v^4 e^{4\lambda(1-v^2)} \frac{U^8(b, 0, \lambda)}{U^8(b, 0, \lambda v^2)} > 0. \quad (4.1)$$

This can be satisfied if the minimum value of the expression (4.1) is strictly positive (on the same interval), thus, we have to analyze the roots of the derivative of expression (4.1),

$$1 - 2\lambda v^2 - 4\lambda v^2 \frac{U'(b, 0, \lambda v^2)}{U(b, 0, \lambda v^2)} = 0, \quad U(b, 0, \lambda v^2) \neq 0, \quad (4.2)$$

where $U'(b, 0, x) = \partial_x U(b, 0, x)$. Denoting

$$x \equiv \lambda v^2, \quad (4.3)$$

the numerical calculations show that the integrals are real-valued if

$$\lambda < x. \quad (4.4)$$

The same conditions can be also derived from the so-called Sonnenschein conditions [19] which state that the g_{00} element of the metric must satisfy

$$\partial_z g_{00}|_{z=z_0} = 0, \quad g_{00}|_{z=z_0} \neq 0, \quad (4.5)$$

in order for the background to be dual to a confining theory in the sense of the area law behavior of a Wilson loop.

The integral (3.16) is the growing function of λ , hence, the large distances correspond to large values of the parameter λ . We get from above that technically the limit $\lambda \rightarrow x$ should be examined in the derivation of the large distance asymptotics. Our procedure includes the following steps. First, we note that the main contribution to the integrals comes from the upper integration bound, $v = 1$, since the integrals diverge in the upper limit. Hence, we should expand the integrands around that point or, rather, the expression under the square root, since other factors under the integral either do not diverge or are constant functions of v . This leads to the expressions,

$$r \underset{v \rightarrow 1}{=} 2\sqrt{\frac{\lambda}{c}} \int_0^1 \frac{dv}{\sqrt{A(b, \lambda)(1-v) + B(b, \lambda)(v-1)^2}}, \quad (4.6)$$

$$E \underset{v \rightarrow 1}{=} \frac{R^2}{\pi\alpha'} \sqrt{\frac{c}{\lambda}} e^{2\lambda} U^4(b, 0, \lambda) \int_0^1 \frac{dv}{\sqrt{A(b, \lambda)(1-v) + B(b, \lambda)(v-1)^2}}, \quad (4.7)$$

where, most notably, the remaining integrals are exactly the same due to identical expressions under the square root. Here the functions $A(b, \lambda)$ and $B(b, \lambda)$ are

$$A(b, \lambda) = -s'_v(b, \lambda; 1) = 4 \left[1 - 2\lambda - 4\lambda \frac{U'(b, 0, \lambda)}{U(b, 0, \lambda)} \right], \quad (4.8)$$

$$B(b, \lambda) = \frac{s''_{vv}(b, \lambda; 1)}{2} = -2 \left[16\lambda^2 - 18\lambda + 3 + 72\lambda^2 \frac{U'(b, 0, \lambda)^2}{U(b, 0, \lambda)^2} + 4\lambda \frac{(16\lambda - 9)U'(b, 0, \lambda) - 2\lambda U''(b, 0, \lambda)}{U(b, 0, \lambda)} \right], \quad (4.9)$$

where

$$s(b, \lambda; v) \equiv 1 - v^4 e^{4\lambda(1-v^2)} \frac{U^8(b, 0, \lambda)}{U^8(b, 0, \lambda v^2)}. \quad (4.10)$$

In the second step, we express the integral in (4.6) via r and substitute it into (4.7). Finally, we take the limit of $\lambda \rightarrow x$ in the found expression and obtain the asymptotics under consideration,

$$E \underset{r \rightarrow \infty}{=} \frac{R^2}{\alpha'} \sigma_\infty r, \quad (4.11)$$

$$\sigma_\infty = \frac{e^{2x} U^4(b, 0, x)}{2\pi x} c. \quad (4.12)$$

As is clear from our discussions above, here $x = x(b)$ represents a non-trivial function of b defined by the Eq. (4.2). In the case of the standard SW model, $b = 0$, one has $x(0) = 1/2$ and the asymptotics (4.12) reduces to the corresponding result of Andreev and Zakharov’s analysis in Ref. [9],

$$\sigma_\infty(0) = \frac{e}{\pi}c \approx 0.87c, \quad (4.13)$$

the relevant details are discussed in the Appendix B. It is known, however, that the simple case of $b = 0$ in (2.11) does not reproduce correctly neither the radial spectrum of light vector mesons nor the pion form-factor. The phenomenology clearly suggests a value of intercept near (see the detailed discussions on this point in Ref. [8])

$$b = -\frac{1}{2}. \quad (4.14)$$

The parameter c can be fixed from the mean slope of Regge like spectra of light mesons found in the compilation [20] (see also the review [21]): $a \approx 1.14 \text{ GeV}^2$. In our further estimates, we will round this value down to $a = 4c = 1.1 \text{ GeV}^2$. Note in passing that the intercept (4.14) in the generalized SW vector spectrum (2.11) leads to the prediction

$$m_\rho^2 = 2c = a/2, \quad (4.15)$$

that correctly reproduces the ρ -meson mass. This is an important phenomenological argument in favor of the physical choice (4.14). It is interesting to note that the relation (4.15) is automatically satisfied in the light-front holographic QCD [10] with the same value of slope $a = 1.1 \text{ GeV}^2$ [22].

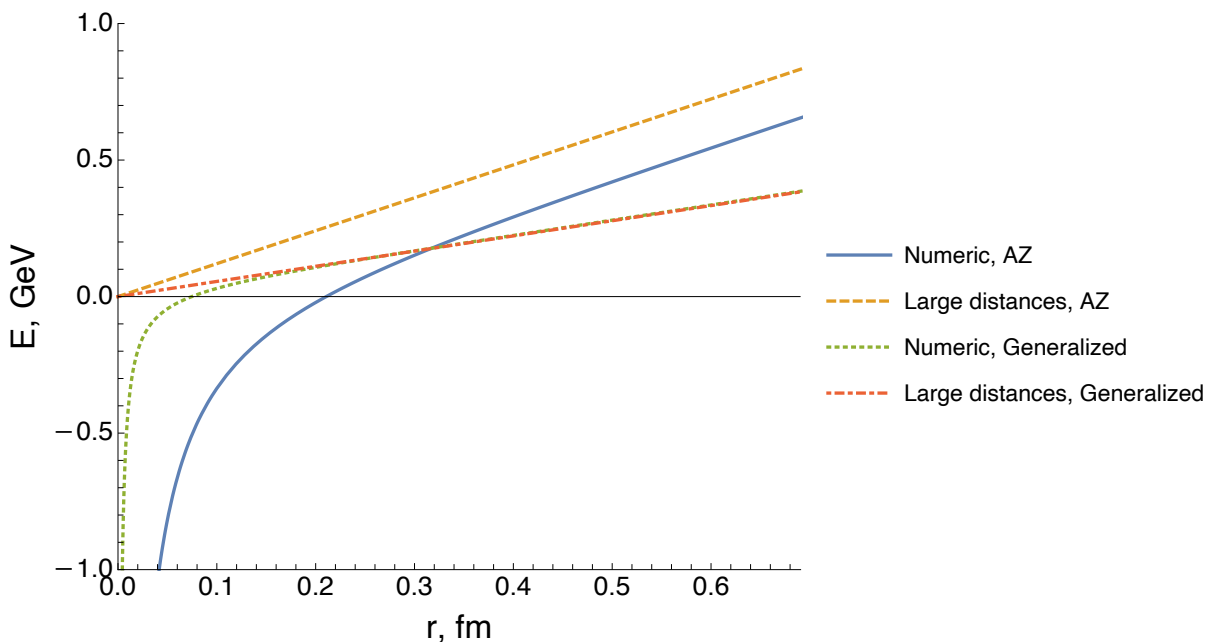


Figure 2: Comparison between the *large* distance asymptotics of the potential and the numerical evaluation of the exact integration formulae (such as (3.16)). “AZ” stands for [9] with adjustments described in the Appendix B, “Generalized” — this work. The parameters are set to: $b = -0.5$, the dilaton parameter to $4c = 1.1 \text{ GeV}^2$, and the normalization constant to $R^2/\alpha' = 1$.

There are several other, unrelated to the holographic QCD, theoretical arguments in favor of the physical choice (4.14), they are discussed in Ref. [8].

Having fixed the parameters we are ready to analyze the impact of non-zero intercept parameter b (which encodes the value of mass gap and likely the effects of the dynamical chiral symmetry breaking [8]) on the large distance asymptotics of the potential in question. The Figure 2 demonstrates the difference between the large distance asymptotics of the potential in the model of [9], corresponding to $b = 0$, and the more physical case corresponding to (4.14). The adjustments needed to take into account the difference in the dilaton background definition in our work and in [9] are described in the Appendix B. In the Figure 2, we also compare the asymptotics with full numerical evaluation of the corresponding original integrals, such as (3.16).

As follows from the plots 2, we obtained a gap between the exact numerical and asymptotic solutions in Andreev–Zakharov’s model [9]. It is seen also that this gap disappears in the physical case of $b = -0.5$. In the general case, the given gap turns out to be b -dependent. We display this dependence in Figure 3. We could not trace analytically the appearance of this discrepancy as a function of b .

In summary, the Figure 2 shows that the incorporation of negative intercept parameter leads to a smaller slope (usually associated with the hadron string tension) of linearly rising confinement potential.

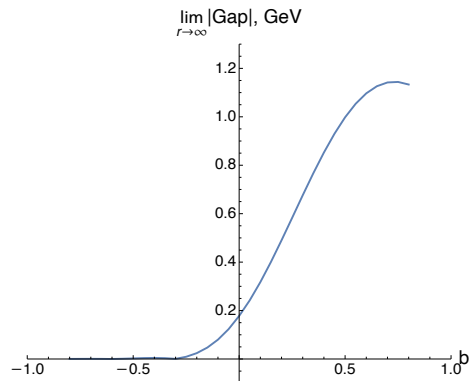


Figure 3: The gap limit at $r \rightarrow \infty$.

5 Small distance potential

Consider now the asymptotics of the energy $E(r)$ at small distances r . Since the distance r is the growing function of λ by virtue of exponents, the small distances correspond to small values of the parameter λ . From (3.7) we can deduce the small λ asymptotics of r by first expanding the integrand at $\lambda \rightarrow 0$

$$r \underset{\lambda \rightarrow 0}{=} 2\sqrt{\frac{\lambda}{c}} \int_0^1 dv \left[\frac{v^2}{\sqrt{1-v^4}} + 2\lambda \left(1 + 2\frac{U'(b, 0, 0)}{U(b, 0, 0)} \right) \frac{v^2(1-v^2)}{(1-v^4)^{3/2}} + O(\lambda^2) \right]. \quad (5.1)$$

Each term in the integral can be integrated separately using the integral representation of the Euler beta-function, as was done, for example, in Ref. [9]. However, instead we would like to take a moment to point out a small subtlety with this integration and perform it more carefully.

First, we should note that the well-known integral representation of the beta-function,

$$B(a, b) \equiv \int_0^1 dt t^{a-1} (1-t)^{b-1},$$

is only valid if both arguments, a and b , are greater than zero, which makes this representation inapplicable in our case, since, as we will show shortly, the arguments can indeed take negative value. Instead, we propose to use the integral representation of the *reduced* beta-function,

$$B_x(a, b) \equiv \int_0^x dt t^{a-1} (1-t)^{b-1}, \quad (5.2)$$

which, in addition, can be defined for negative values of the second argument b as long as $x < 1$. We perform the actual integration with the use of the shorthand formula

$$\int_0^1 dv v^a (1-v^4)^b = \frac{1}{4} \lim_{x \rightarrow 1} B_x \left(\frac{a+1}{4}, b+1 \right), \quad (5.3)$$

which yields

$$r \underset{\lambda \rightarrow 0}{=} \frac{1}{2} \sqrt{\frac{\lambda}{c}} \lim_{x \rightarrow 1} \left[B_x \left(\frac{3}{4}, \frac{1}{2} \right) + \lambda \left(1 + 2 \frac{U'(b, 0, 0)}{U(b, 0, 0)} \right) \left(B_x \left(\frac{3}{4}, -\frac{1}{2} \right) - B_x \left(\frac{5}{4}, -\frac{1}{2} \right) \right) \right]. \quad (5.4)$$

In order to take the limit we make use of the expansion of the reduced beta-function

$$B_x(a, b) \underset{x \rightarrow 1}{=} B(a, b) - \frac{(1-x)^b}{b} + O\left((x-1)^{b+1}\right), \quad (5.5)$$

where the beta-function $B(a, b)$ represents the standard combination of the gamma-functions,

$$B(a, b) = \frac{\Gamma(a)\Gamma(b)}{\Gamma(a+b)}. \quad (5.6)$$

It is seen immediately that the first term in (5.4) reduces to the normal beta-function and, more importantly, the divergences from the second and the third terms cancel each other out. Note that while in this particular case it does not make difference, this subtle detail would have been missed if we had used the normal beta-function instead of the reduced one from the beginning.

In the final step, using the standard properties of the beta- and gamma-functions and introducing a new parameter

$$\rho \equiv \frac{\Gamma\left(\frac{1}{4}\right)^2}{(2\pi)^{3/2}}, \quad (5.7)$$

we obtain the small- λ expansion of the distance

$$r \underset{\lambda \rightarrow 0}{=} \frac{1}{\rho} \sqrt{\frac{\lambda}{c}} \left[1 + \lambda \left(1 + 2 \frac{U'(b, 0, 0)}{U(b, 0, 0)} \right) (\pi\rho^2 - 1) \right]. \quad (5.8)$$

The small- λ asymptotics of the integral for the energy (3.14) can be analyzed in a similar manner. The final result is

$$E \underset{\lambda \rightarrow 0}{=} \frac{R^2}{2\pi\alpha'\rho} U^4(b, 0, 0) \sqrt{\frac{c}{\lambda}} \left[-1 + \lambda \left(1 + 2 \frac{U'(b, 0, 0)}{U(b, 0, 0)} \right) (3\pi\rho^2 - 1) \right]. \quad (5.9)$$

The explicit formulae for the intermediate steps of this computation can be found in the Appendix A.

In order to obtain the small distance potential we combine the last two expressions by expressing λ in terms of r . First, we extract from (5.8)

$$\sqrt{\frac{c}{\lambda}} = \frac{1}{\rho r} \left[1 + \lambda \left(1 + 2 \frac{U'(b, 0, 0)}{U(b, 0, 0)} \right) (\pi\rho^2 - 1) \right], \quad (5.10)$$

which we substitute back into the asymptotics (5.9) for the energy

$$E \underset{\lambda \rightarrow 0}{=} \frac{R^2}{2\pi\alpha'\rho} \frac{U^4(b, 0, 0)}{\rho r} \left[1 + \lambda \left(1 + 2 \frac{U'(b, 0, 0)}{U(b, 0, 0)} \right) (\pi\rho^2 - 1) \right] \times \\ \times \left[-1 + \lambda \left(1 + 2 \frac{U'(b, 0, 0)}{U(b, 0, 0)} \right) (3\pi\rho^2 - 1) \right]. \quad (5.11)$$

Next, we perform the multiplication of the square brackets while retaining only the terms up to quadratic in λ ,

$$E \underset{\lambda \rightarrow 0}{=} \frac{R^2}{2\pi\alpha'\rho} \frac{U^4(b, 0, 0)}{\rho r} \left[-1 + \lambda \left(1 + 2 \frac{U'(b, 0, 0)}{U(b, 0, 0)} \right) (-\pi\rho^2 + 1 + 3\pi\rho^2 - 1) \right] = \\ = \frac{R^2}{2\pi\alpha'\rho} \frac{U^4(b, 0, 0)}{\rho r} \left[-1 + 2\pi\rho^2\lambda \left(1 + 2 \frac{U'(b, 0, 0)}{U(b, 0, 0)} \right) \right]. \quad (5.12)$$

Finally, we express from (5.10) in the leading order

$$\lambda = c\rho^2 r^2, \quad (5.13)$$

substitute this into (5.12), perform some simplifications, and we get

$$E \underset{r \rightarrow 0}{=} \frac{R^2}{\alpha'} U^4(b, 0, 0) \left[-\frac{1}{2\pi\rho^2} \frac{1}{r} + \left(1 + 2 \frac{U'(b, 0, 0)}{U(b, 0, 0)} \right) c\rho^2 r \right]. \quad (5.14)$$

This result can be simplified even further by using the properties of the Tricomi function. First, we note that

$$U(b, k, 0) = \frac{\Gamma(1-k)}{\Gamma(b-k+1)}, \quad \text{if } k < 1, \quad (5.15)$$

which means that

$$U^4(b, 0, 0) = \frac{1}{\Gamma(1+b)^4}. \quad (5.16)$$

Secondly, using various known series expansions of the Tricomi function we can write

$$1 + 2 \frac{U'(b, 0, 0)}{U(b, 0, 0)} = 1 + 2b\psi(b+1) + 4b\gamma + 2b \log \varepsilon, \quad (5.17)$$

where $\varepsilon \rightarrow 0$. Here ψ is the digamma function and γ is Euler's constant. The last diverging constant appears from the expansion of $U'(b, 0, \varepsilon)$ at small ε . Combining these expressions we obtain

$$E \underset{r \rightarrow 0}{=} \frac{R^2}{\alpha'} \left[-\frac{\kappa_0}{r} + \sigma_0 r \right], \quad (5.18)$$

$$\kappa_0 \equiv \frac{1}{\Gamma(1+b)^4} \frac{1}{2\pi\rho^2}, \quad \sigma_0 \equiv \frac{1 + 2b\psi(b+1) + 4b\gamma}{\Gamma(1+b)^4} c\rho^2. \quad (5.19)$$

Note that in the relation (5.18) we subtracted the logarithmic divergence in the expansion (5.17) arising from the limit of $\lambda \rightarrow 0$ in our notation. The expression (5.18) represents, thus, the *renormalized* energy.

Let us now compare the small distance potential (5.18) with the one obtained in [9]. As in the previous section, for the latter we use the adjusted formulae which are presented in the Appendix B. The comparison is given in the Figure 4. As a benchmark we also demonstrate

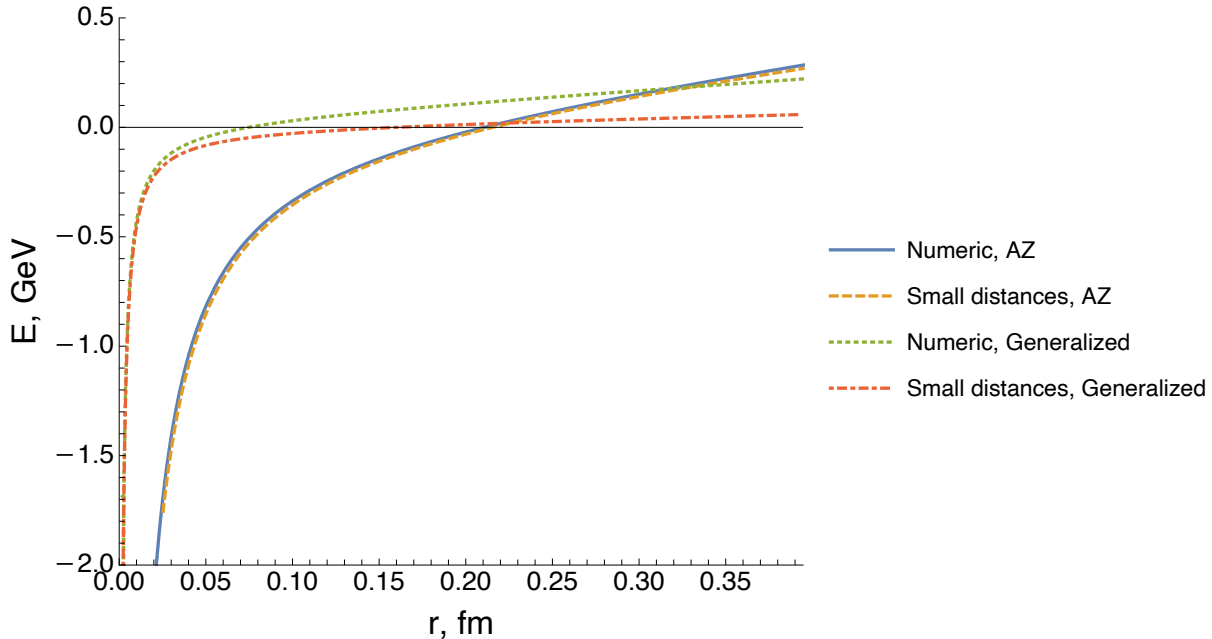


Figure 4: Comparison between the *small* distance asymptotics of the potential and the numerical evaluation of the exact integration formulae (such as (3.16)). “AZ” stands for [9] with adjustments described in the Appendix B, “Generalized” — this work. The parameters are set to: $b = -0.5$, the dilaton parameter to $4c = 1.1 \text{ GeV}^2$, and the normalization constant to $R^2/\alpha' = 1$.

the results of the numerical evaluation of the corresponding exact formulae for $r(\lambda)$ and $E(\lambda)$. One can note that the gap between asymptotics and numerical results that we observed for large distances for the model of [9] disappears at small distances. Additionally, the small distance potential asymptotics in the current model reproduce the “exact” solutions quite well.

In summary, the Figure 4 demonstrates that the Coulomb part of the potential comes into play at smaller distances if the intercept parameter b is negative. For instance, if we set the normalization constant to $R^2/\alpha' = 1$ as in the Figure 4 then in the Andreev–Zakharov’s model, defined at $b = 0$, the Coulomb part becomes substantial at a distance less than 0.1 fm while in the considered phenomenologically preferable case of $b = -0.5$, this distance drops to about 0.03 fm.

6 The scalar case

Let us now apply the analysis above to the scalar case. In this case, the analogue of the generalized SW action (2.12) reads [8]

$$S_{\text{sc}} = \int d^4x dz \sqrt{g} e^{-cz^2} U^2(b, -1, |cz^2|) \mathcal{L}_{\text{sc}}. \quad (6.1)$$

The mass spectrum of the SW model (6.1) with $c > 0$ is [8, 23]

$$m_n^2 = 4c(n + \Delta/2 + b), \quad n = 0, 1, 2, \dots, \quad (6.2)$$

where Δ is the canonical dimension of QCD scalar operator dual to the corresponding 5D scalar field in the Lagrangian density \mathcal{L}_{sc} .

As in the vector case, for our purposes one should rewrite the dilaton background as certain modification of AdS₅ metric using (2.15) and continue the modified metric to the Euclidean space. The background function $h(z)$ of the metric in (3.15) is then replaced by (see also discussions in [18])

$$h = e^{2cz^2/3} U^{4/3}(b, -1, cz^2) = e^{2\lambda v^2/3} U^{4/3}(b, -1, \lambda v^2). \quad (6.3)$$

This changes the expressions for $r(\lambda)$ and $E(\lambda)$ to the following ones,

$$r = 2\sqrt{\frac{\lambda}{c}} \int_0^1 dv \frac{U^{4/3}(b, -1, \lambda)}{U^{4/3}(b, -1, \lambda v^2)} \frac{v^2 e^{2\lambda(1-v^2)/3}}{\sqrt{1 - v^4 e^{4\lambda(1-v^2)/3} \frac{U^{8/3}(b, -1, \lambda)}{U^{8/3}(b, -1, \lambda v^2)}}}, \quad (6.4)$$

$$E = \frac{R^2}{\pi\alpha'} \sqrt{\frac{c}{\lambda}} \left[\int_0^1 \frac{dv}{v^2} \left(\frac{e^{2\lambda v^2/3} U^{4/3}(b, -1, \lambda v^2)}{\sqrt{1 - v^4 e^{4\lambda(1-v^2)/3} \frac{U^{8/3}(b, -1, \lambda)}{U^{8/3}(b, -1, \lambda v^2)}}} - D \right) - D \right], \quad (6.5)$$

with the regularization constant $D \equiv U^{4/3}(b, -1, 0)$.

The derivation of the asymptotics in question is essentially the same. For the large distance asymptotics we get

$$E \underset{r \rightarrow \infty}{=} \frac{R^2}{\alpha'} \sigma_\infty r, \quad (6.6)$$

$$\sigma_\infty = \frac{e^{2x/3} U^{4/3}(b, -1, x)}{2\pi x} c, \quad (6.7)$$

where x (see (4.3)) is now the solution to the equation

$$1 - \frac{2}{3}x - \frac{4}{3}x \frac{U'(b, -1, x)}{U(b, -1, x)} = 0, \quad (6.8)$$

which is the scalar counterpart of Eq. (4.2). In the case of the standard SW model, $b = 0$, we get $x(0) = 3/2$. Comparing (6.7) with (4.12) at $b = 0$ we have $\sigma_\infty^{(\text{sc})}/\sigma_\infty^{(\text{vec})} = 1/3$. The emerging factor of 1/3 stems from the appearance of the additional factor of 1/3 in the exponent of scalar background function (6.3) in comparison with (3.15). The given factor provides the equal slope of scalar and vector radial Regge trajectories in the SW model.

The details of the derivation of the small distance asymptotics are given in the Appendix A, the result is

$$E \underset{r \rightarrow 0}{=} \frac{R^2}{\alpha'} U^{4/3}(b, -1, 0) \left[-\frac{1}{2\pi\rho^2} \frac{1}{r} + \left(1 + 2 \frac{U'(b, -1, 0)}{U(b, -1, 0)} \right) \frac{c\rho^2}{3} r \right]. \quad (6.9)$$

It can be simplified using the analogous to (5.17) expansion,

$$1 + 2 \frac{U'(b, -1, 0)}{U(b, -1, 0)} = 1 - 2b, \quad (6.10)$$

where in contrast to the vector case the logarithmic term has the form of $\varepsilon \log \varepsilon$ that goes to 0 as $\varepsilon \rightarrow 0$. Finally, we obtain

$$E \underset{r \rightarrow 0}{=} \frac{R^2}{\alpha'} \left[-\frac{\kappa_0}{r} + \sigma_0 r \right], \quad (6.11)$$

$$\kappa_0 = \frac{1}{\Gamma(2+b)^{4/3}} \frac{1}{2\pi\rho^2}, \quad \sigma_0 = \frac{1-2b}{\Gamma(2+b)^{4/3}} \frac{c\rho^2}{3}. \quad (6.12)$$

It is interesting to note that in the scalar case, the logarithmic divergence from the derivative of the Tricomi in (6.10) is absent, i.e., the asymptotics (6.9) does not need the renormalization caused by the subtraction of that divergence.

7 Discussions

For a phenomenological analysis of our results we should first provide a very brief review of the relevant phenomenology of the Cornell potential (1.1). Let us write this potential once more for a further convenience,

$$V(r) = -\frac{\kappa}{r} + \sigma r + C. \quad (7.1)$$

In typical potential models for heavy quarkonia (for a review see, e.g., [1]), the constant C is roughly $C \approx -0.3$ GeV. The potential (7.1) was first proposed in Ref. [2] for a non-relativistic description of the charmonia spectrum. The linear confinement potential at large distances was inferred from lattice gauge theory and also inspired by the dual string model [24–27]. The spin averaged charmonia spectrum (plus ground states of bottomonia) results in parameter values [1]

$$\text{Charmonia:} \quad \kappa \approx 0.25, \quad \sigma \approx 0.21 \text{ GeV}^2. \quad (7.2)$$

The perturbative QCD predicts the value of Coulomb coefficients for quarkonia,

$$\kappa = \frac{4}{3}\alpha_s(r), \quad (7.3)$$

where $\alpha_s(r)$ is the QCD running coupling which depends on renormalization scheme. The renormalization scheme to be used with the potential is the so-called V-scheme which is determined by perturbative high order QCD corrections to the static potential (see, e.g., Refs. [28, 29] for relevant discussions). In the case of Cornell potential, however, the scale for $\alpha_s(r)$ is not well-defined and the coefficient κ of the Coulomb-like part is related with an average value $\langle\alpha_s\rangle$ over the scale range where that part of the potential is dominant. The mean value of the coupling $\langle\alpha_s\rangle$ depends on the size of the hadrons considered. The value of $\langle\alpha_s\rangle$ extracted in Ref. [2] from hadronic decays of excited charmonia is $\langle\alpha_s(\psi)\rangle = 0.19 \pm 0.03$. This value is consistent with (7.2) and (7.3): $\frac{4}{3}0.19 \approx 0.25$. After inclusion of excited bottomonia, that probe the potential at smaller distances, the estimates (7.2) were shifted to the following approximate values [1],

$$\text{Charmonia + Bottomonia:} \quad \kappa \approx 0.51, \quad \sigma \approx 0.18 \text{ GeV}^2. \quad (7.4)$$

In the region $0.2 \text{ fm} < r < 1 \text{ fm}$, which is effectively probed by spin-averaged quarkonia splittings, the parametrizations (7.2) and (7.4), however, differ only marginally: The higher value of the Coulomb coefficient is compensated for by a smaller slope σ [1].

The value of slope σ in (7.4) turns out to be remarkably insensitive to a chosen distance. The same value is typically used for the description of the light meson spectrum within the potential models¹. Even more surprising is the quantitative agreement of the mean slope of Regge spectra

¹With certain model modifications like a smearing procedure in the coordinate space to take into account relativistic effects and the use of an *ad hoc* model for the running coupling that freezes out at low energies, the paper [30] is a classical work in this field.

of light mesons, $a \approx 1.14 \text{ GeV}^2$ [20], with the slope predicted by semiclassical quantization of hadron string with linearly rising potential energy (7.1), $a = 2\pi\sigma$, where σ is the string tension (see, e.g., the discussions in Ref. [21]), if the value from (7.4) is used for σ .

After this brief reminder, we are ready to analyze the relevant phenomenological predictions of our generalized SW holographic model. First of all, it should be noted that the coupling of the Coulomb-like part of the potential obtained within the holographic approach is not running at large energy-momenta because this approach represents a classical framework. On the other hand, it can run at the low energy-momenta due to semiclassical effects that are part of the definition of the coupling [11]. Therefore, the constant coupling should be understood as the value averaged over energy-momentum of the actually running coupling. With this in mind, comparing directly our results to that of the Cornell potential is self-consistent.

Let us consider the predictions which do not depend on the general normalization constant R^2/α' . We can temporarily set $R^2/\alpha' = 1$, then our definitions of parameters κ and σ coincide with the definitions in the Cornell potential (7.1). The first prediction is the ratio σ_∞/κ_0 . In the vector case, we obtain from (4.12) and (5.19)

$$\frac{\sigma_\infty}{\kappa_0} = \frac{\Gamma\left(\frac{1}{4}\right)^4 \Gamma(1+b)^4 e^{2x} U(b, 0, x)^4 c}{(2\pi)^3 x}. \quad (7.5)$$

Andreev and Zakharov got the estimate $\sigma_\infty/\kappa_0 \approx 0.85 \text{ GeV}^2$ [9] and found it “disappointing” that this prediction disagreed significantly with the corresponding phenomenological ratio from (7.4),

$$\text{Charmonia + Bottomonia:} \quad \frac{\sigma}{\kappa} \approx 0.35 \text{ GeV}^2. \quad (7.6)$$

We should note, however, that in the fit (7.2) this ratio is equal to 0.84 in nice agreement with the Andreev–Zakharov prediction. Taking into account the aforementioned remark on a phenomenological proximity of the parametrizations (7.2) and (7.4), the obtained estimate looks reasonable².

The general behavior of ratio σ_∞/κ_0 as a function of intercept parameter b in the vector and scalar case is displayed in the Figure 5. It is seen that the physical value of intercept in the vector case, $b \approx -0.5$, leads to an unrealistically large ratio, while the scalar case with $b \approx 0$ is perfectly compatible with the phenomenological output (7.6).

The next important ratio is σ_∞/σ_0 which does not depend on the Regge slope $a = 4c$. The lattice data suggest that the linearly rising part in the Cornell potential (7.1) is almost universal at large and small distances, hence, a reasonable prediction for σ_∞/σ_0 should lie near 1 [9]. The prediction of Andreev–Zakharov model is $\sigma_\infty/\sigma_0 \approx 1.24$ [9] that corresponds to $b = 0$ in our model. The general behavior of ratio σ_∞/σ_0 as a function of b is displayed in the Figure 5. In the same Figure, we show the corresponding behavior in the scalar SW model. It is seen that the physical value of intercept in the vector case, $b \approx -0.5$, leads to an unrealistically large ratio, while the scalar case gives a stable prediction near 1 for $b \lesssim 0$.

Our further predictions will depend on the choice of normalization constant R^2/α' . First let us assume that this constant is b -independent. Without loss of generality, we may again set $R^2/\alpha' = 1$. The slope σ is a function of b . Since the intercept b encodes important physics of non-perturbative strong interactions, it is interesting to check the behavior of $\sigma(b)$ at large and small distances since this reflects the dependence on b of string tension and of the slope of the

²We should mention, however, that the value of Regge slope was set in [9] equal to $a = 4c = 0.9 \text{ GeV}^2$. With our value of $4c = 1.1 \text{ GeV}^2$, the relation (7.5) for $b = 0$ would give $\sigma_\infty/\kappa_0 \approx 1.04 \text{ GeV}^2$, see also the Figure 5.

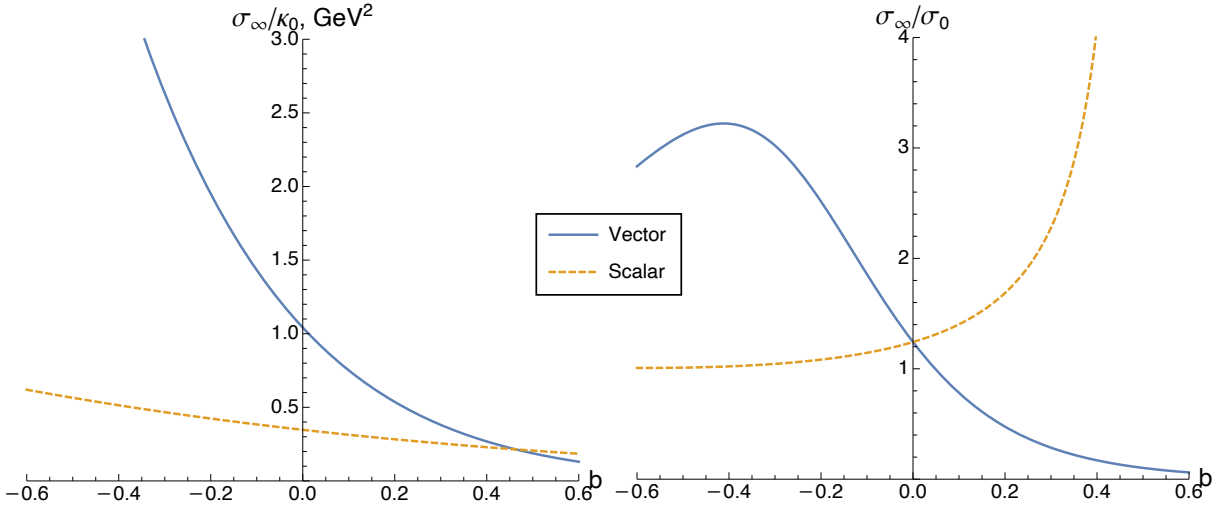


Figure 5: The ratios σ_∞/κ_0 (left) and σ_∞/σ_0 (right) in the vector and scalar cases. The Regge slope is set to $4c = 1.1 \text{ GeV}^2$.

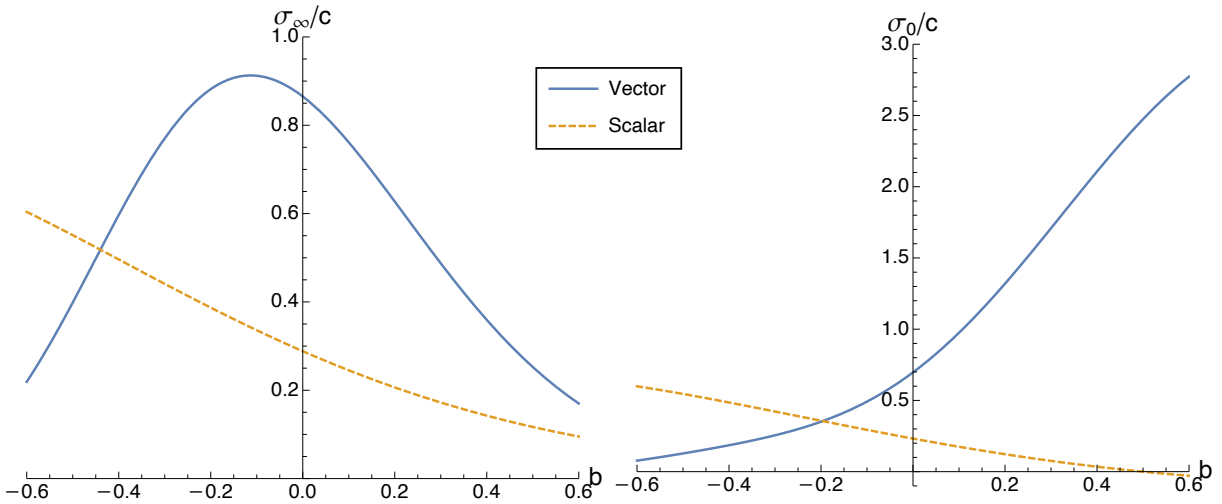


Figure 6: The ratios σ_∞/c (left) and σ_0/c (right) in the vector and scalar cases.

Regge spectrum. In the Figure 6, we show the dependence on b of c -independent ratios σ_∞/c and σ_0/c in the vector and scalar SW models. One can conclude from the presented plots that the behavior of $\sigma_\infty(b)$ and $\sigma_0(b)$ is qualitatively similar in the scalar case and is very different in the vector one.

Now let us relax the assumption above. The dependence of the normalization constant R^2/α' on b can help to amend the following theoretical discrepancy. As was mentioned above, the semiclassical quantization of hadron string of the Nambu-Goto type with tension σ and linearly growing with distance energy as in (7.1), leads to the slope of the angular and radial Regge mass spectrum $a = 2\pi\sigma$. On the other hand, the same slope in the SW holographic model is $a = 4c$, see, e.g., the SW spectrum (2.9) or (6.2). The physical values of σ and c remarkably agree with each other. But this agreement can be destroyed by the dependence $\sigma(b)$ as long as the parameter c in the SW model does not depend on b . And here the normalization constant

R^2/α' can restore the consistency: The actual σ in (7.1) is our $\frac{R^2}{\alpha'}\sigma_\infty$, hence, we may impose the consistency condition,

$$\frac{R^2}{\alpha'} 2\pi\sigma_\infty(b) = 4c, \quad (7.7)$$

that should fix the normalization constant R^2/α' . For instance, in the vector SW model at $b = 0$, we get from (4.13) and (7.7) the normalization $R^2/\alpha' = 2/e \approx 0.74$. The given normalization constant is not very distinct from $R^2/\alpha' = 1$ used in our work.

When the normalization (7.7) is imposed, the string tension σ in the confinement potential (7.1) does not depend on the intercept parameter b while the Coulomb parameter κ and constant C are functions of b . Their b -dependence can be calculated numerically, we display the result in the Figure 7. These plots show that the physical value of intercept in the vector case, $b \approx -0.5$, leads to an unrealistically small value of κ and to positive C , while the scalar case with $b \approx 0$ reproduces numerically the value of κ in the phenomenological fit (7.4) and qualitatively gives the correct sign of constant C .

It is interesting to compare our models normalized by the condition (7.7) with the results of lattice simulations in $SU(3)$ gauge theory. In the Figure 8, we provide such a comparison for three typical cases: The vector SW model with $b = 0$ (the simplest standard variant), with $b = -0.5$ (the phenomenologically preferable variant (4.14)), and the scalar SW model with $b = 0$ (the most consistent variant according to our analysis).

In summary, the totality of observations made above shows that the holographic confinement potential quantitatively compatible with the phenomenology arises in the *scalar* version of the SW holographic model, in which the physical value of intercept parameter b in the Regge-like spectrum (6.2) seems to be close to zero.

The latter observation could be converted into a prediction for the mass m_s of ground scalar state. If the quark physical degrees of freedom are quenched, only the gluon ones are operative. The minimal dimension of scalar operator constructed from the gluon fields is $\Delta = 4$ (the scale-invariant operator $\beta G_{\mu\nu}^2$). Then the spectrum (6.2) with $b \approx 0$ combined with the relation (4.15)

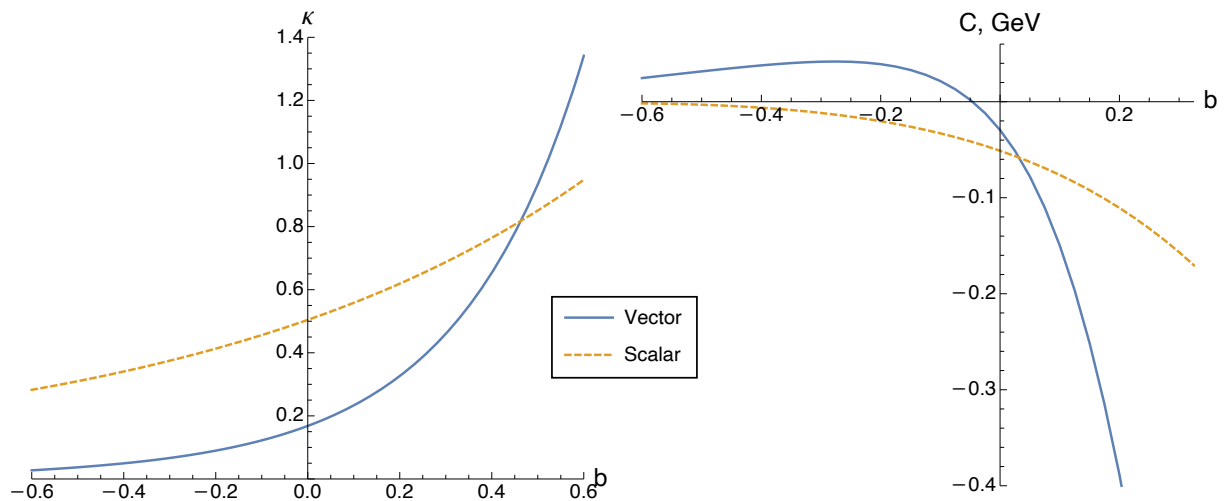


Figure 7: The behavior of the parameters κ (left) and C (right) in the potential (7.1) as functions of the intercept b when the normalization (7.7) is imposed. The Regge slope is set to $4c = 1.1 \text{ GeV}^2$ (equivalently, $\sigma_\infty = 0.18 \text{ GeV}^2$).

leads to the following prediction for the mass of the lightest scalar glueball,

$$m_s \approx 2m_\rho. \quad (7.8)$$

This prediction is close to the mass of the scalar meson $f_0(1500)$ which is indeed a candidate for the lightest scalar glueball [31].

8 Conclusions

The Soft Wall AdS/QCD approach provides a natural framework for the appearance of the Cornell type confinement potential at short and long distances. We performed a detailed analytical study of arising confinement potentials within the generalized version of Soft Wall holographic model in the vector and scalar cases, where the term “generalized” means the incorporation of arbitrary intercept into the radial Regge spectrum. The intercept parameter is indispensable for a quantitative phenomenological description of the experimental spectrum of light meson resonances. Our numerical analysis and comparison with the phenomenological Cornell potentials showed that quantitatively correct confinement potential arises in a consistent way within the scalar Soft Wall holographic model, while the standard vector version of the model results in a qualitative agreement only. This conclusion agrees with the recent analysis of Ref. [32] where it was argued that quantitatively correct prediction of the deconfinement temperature within the framework of the same model emerges in the scalar case. And as in Ref. [32], the found numerical parameters seem to be consistent with the interpretation of the scalar state $f_0(1500)$ [31] as the lightest glueball.

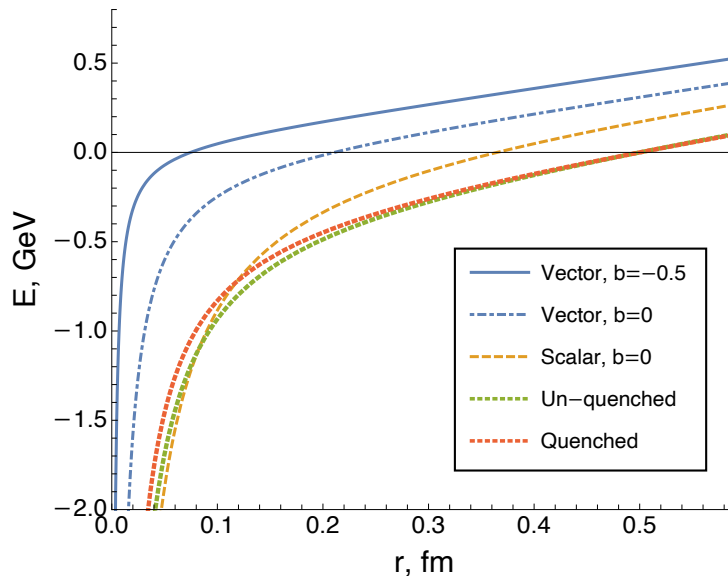


Figure 8: The behavior of potential energy with distance for three examples of SW holographic model discussed in the text. The lattice data for the Wilson action $SU(3)$ potential are taken from the review [1]. More precisely, we made use of the Cornell potential (7.1) that almost perfectly interpolates these data, the parameters of this potential are the following [1]: $\sigma = 0.18 \text{ GeV}^2$, $\kappa = 0.295$ for the quenched approximation and $\kappa \approx 0.36$ in the un-quenched case (sea quarks effects are taken into account), in both cases the constant C is fixed by the condition $E(0.5 \text{ fm}) = 0$.

We have no clear understanding on why the scalar version of considered generalized SW holographic model is quantitatively more consistent with the phenomenology of quark confinement than the vector one. But we see here the manifestation of a general tendency for the dominance of the vacuum scalar sector in the non-perturbative dynamics of strong interactions. This dominance is ubiquitous: The universality of hadron-hadron scattering at ultrahigh energies is believed to be associated with the exchange of scalar pomerons, and not vector gluons, as one might naively expect; in the opposite limit of very low energies, the predominant part of attraction potential between nucleons is due to the exchange of scalar σ -meson [31] (a correlated two-pion exchange), and not pseudoscalar π -mesons, as one could naively expect; at intermediate energies, the number of observed scalar isoscalar resonances [31] is much greater than it should follow from the quark model...

In summary, we believe that our results provide a new demonstration of the key role of the vacuum scalar sector in the description of confinement physics in strong interactions.

Acknowledgements

This research was funded by the Russian Science Foundation grant number 21-12-00020.

Appendices

A Details of the small distance asymptotics calculation

In this Appendix, we present technical details concerning the derivation of the small distance asymptotics.

First we consider the small- λ asymptotics of the energy integral (3.14) for the vector case. The expansion of its integrand at $\lambda \rightarrow 0$, where we also substitute the regularization constant $D = U^4(b, 0, 0)$, reads

$$E \underset{\lambda \rightarrow 0}{=} \frac{R^2}{\pi \alpha'} \sqrt{\frac{c}{\lambda}} \left[\int_0^1 \frac{dv}{v^2} (E_0 + \lambda E_1 + O(\lambda^2)) - U^4(b, 0, 0) \right]. \quad (\text{A.1})$$

Here we introduced the expansion coefficients

$$E_0 \equiv U^4(b, 0, 0) \left(\frac{1}{\sqrt{1-v^4}} - 1 \right), \quad (\text{A.2})$$

$$E_1 \equiv 2U^4(b, 0, 0) \left(1 + 2 \frac{U'(b, 0, 0)}{U(b, 0, 0)} \right) \frac{v^2(1-2v^4+v^2)}{(1-v^4)^{3/2}}. \quad (\text{A.3})$$

On the next step, the E_0 and E_1 terms are integrated using the integral representation of the reduced beta-function (5.3). Note, however, that technically E_0 contains two integrals and both of them are divergent. Below we show a trick which we use to demonstrate that these divergences cancel each other out. We start by rewriting the integrals as

$$\int_0^1 \frac{dv}{v^2} \left(\frac{1}{\sqrt{1-v^4}} - 1 \right) = \lim_{\substack{x \rightarrow 1 \\ y \rightarrow 0}} \int_y^x \frac{dv}{v^2} \left(\frac{1}{\sqrt{1-v^4}} - 1 \right) = \dots \quad (\text{A.4})$$

After that we change the integration variable to $u \equiv v^4$ and split the first integral into two

$$\dots = \frac{1}{4} \lim_{\substack{x \rightarrow 1 \\ y \rightarrow 0}} \left(\int_0^{x^4} du \frac{u^{-5/4}}{\sqrt{1-u}} - \int_0^{y^4} du \frac{u^{-5/4}}{\sqrt{1-u}} - \int \frac{du}{y^4} \right) = \dots \quad (\text{A.5})$$

We can now safely perform the integration (for the first two integrals we use the integral representation (5.3) of the reduced beta-function) and we get

$$\dots = \frac{1}{4} \lim_{\substack{x \rightarrow 1 \\ y \rightarrow 0}} \left[B_{x^4} \left(-\frac{1}{4}, \frac{1}{2} \right) - B_{y^4} \left(-\frac{1}{4}, \frac{1}{2} \right) + \frac{4}{x} - \frac{4}{y} \right] = \dots \quad (\text{A.6})$$

Using the expansions of the reduced beta-function (5.5) and

$$B_y(a, b) \underset{y \rightarrow 0}{=} \frac{y^a}{a} + O(y^{a+1}), \quad (\text{A.7})$$

we obtain

$$\dots = \frac{1}{4} \lim_{\substack{x \rightarrow 1 \\ y \rightarrow 0}} \left[B \left(-\frac{1}{4}, \frac{1}{2} \right) - 2\sqrt{1-x^4} + O\left((1-x^4)^{3/2}\right) + \frac{4}{y} + O(y^3) + \frac{4}{x} - \frac{4}{y} \right] = \dots, \quad (\text{A.8})$$

from which we immediately see that the divergences indeed cancel each other out and the final result of the integration of E_0 is

$$\int_0^1 \frac{dv}{v^2} E_0 = U^4(b, 0, 0) \left[\frac{1}{4} B \left(-\frac{1}{4}, \frac{1}{2} \right) + 1 \right]. \quad (\text{A.9})$$

The integral for E_1 can be represented as three separate integrals,

$$\int_0^1 \frac{dv}{v^2} E_1 = 2U^4(b, 0, 0) \left(1 + 2 \frac{U'(b, 0, 0)}{U(b, 0, 0)} \right) \int_0^1 dv \frac{1 - 2v^4 + v^2}{(1 - v^4)^{3/2}}, \quad (\text{A.10})$$

each of which results in the beta-function. The end result for E_1 is

$$\int_0^1 \frac{dv}{v^2} E_1 = \frac{U^4(b, 0, 0)}{2} \left(1 + 2 \frac{U'(b, 0, 0)}{U(b, 0, 0)} \right) \left[B \left(\frac{1}{4}, -\frac{1}{2} \right) + B \left(\frac{3}{4}, -\frac{1}{2} \right) - 2B \left(\frac{5}{4}, -\frac{1}{2} \right) \right]. \quad (\text{A.11})$$

We can now substitute (A.9) and (A.11) back into (A.1) (note that the out-of-integral $U^4(b, 0, 0)$ terms cancel each other out) and use the properties of the gamma-functions as well as the definition (5.7) of ρ . This leads to the final form (5.9) for the small- λ asymptotics of energy.

The calculations in the scalar case are similar — we have to adjust only the coefficients in front of the integrals, which give rise to the beta-functions. The small λ expansion of the integral (6.4) for the distance is equal to

$$r \underset{\lambda \rightarrow 0}{=} 2\sqrt{\frac{\lambda}{c}} \int_0^1 dv \left[\frac{v^2}{\sqrt{1-v^4}} + \frac{2}{3}\lambda \left(1 + 2 \frac{U'(b, -1, 0)}{U(b, -1, 0)} \right) \frac{v^2(1-v^2)}{(1-v^4)^{3/2}} + O(\lambda^2) \right]. \quad (\text{A.12})$$

For the energy integral (6.5) we use the same form of the expansion,

$$E \Big|_{\lambda \rightarrow 0} = \frac{R^2}{\pi\alpha'} \sqrt{\frac{c}{\lambda}} \left[\int_0^1 \frac{dv}{v^2} (E_0 + \lambda E_1 + O(\lambda^2)) - U^{4/3}(b, -1, 0) \right], \quad (\text{A.13})$$

with redefined expansion coefficients

$$E_0 \equiv U^{4/3}(b, -1, 0) \left(\frac{1}{\sqrt{1-v^4}} - 1 \right), \quad (\text{A.14})$$

$$E_1 \equiv \frac{2}{3} U^{4/3}(b, -1, 0) \left(1 + 2 \frac{U'(b, -1, 0)}{U(b, -1, 0)} \right) \frac{v^2(1-2v^4+v^2)}{(1-v^4)^{3/2}}. \quad (\text{A.15})$$

Then the remaining integrals can be computed just as they were for the vector case and this results in (6.9).

For completeness, we present those properties of gamma-functions which were used in the calculations above,

$$\Gamma\left(\frac{1}{2}\right) = \sqrt{\pi}, \quad \Gamma\left(\frac{3}{4}\right) \Gamma\left(\frac{1}{4}\right) = \pi\sqrt{2}, \quad \Gamma(z+1) = z\Gamma(z), \quad \Gamma\left(-\frac{1}{2}\right) = -2\sqrt{\pi}. \quad (\text{A.16})$$

B Adjustments to earlier results

In this Appendix, we review the adjustments to the results from [9] that are required in order to make a meaningful comparison. The starting point is the integral representation of the potential in terms of the parametric functions $r(\lambda)$ and $E(\lambda)$ (counterparts to our (3.16) and (3.17)),

$$r = 2\sqrt{\frac{\lambda}{c}} \int_0^1 dv \frac{v^2 e^{\lambda(1-v^2)/2}}{\sqrt{1-v^4 e^{\lambda(1-v^2)}}},$$

$$E = \frac{R^2}{\pi\alpha'} \sqrt{\frac{c}{\lambda}} \left[\int_0^1 \frac{dv}{v^2} \left(\frac{e^{\lambda v^2/2}}{\sqrt{1-v^4 e^{\lambda(1-v^2)}}} - 1 \right) - 1 \right].$$

The pertinent difference between [9] and the current work is the difference in the definitions of the exponential background in the AdS₅ metric: $e^{cz^2/2}$ vs. e^{2cz^2} , correspondingly. This implies that in order to use the above two formulae we have to substitute $c \rightarrow 4c$ and, consequently, $\lambda \rightarrow 4\lambda$ due to its definition, $\lambda \equiv cz_0^2$. The integrals for the distance and energy change to the following ones,

$$r = 2\sqrt{\frac{\lambda}{c}} \int_0^1 dv \frac{v^2 e^{2\lambda(1-v^2)}}{\sqrt{1-v^4 e^{4\lambda(1-v^2)}}}, \quad (\text{B.1})$$

$$E = \frac{R^2}{\pi\alpha'} \sqrt{\frac{c}{\lambda}} \left[\int_0^1 \frac{dv}{v^2} \left(\frac{e^{2\lambda v^2}}{\sqrt{1-v^4 e^{4\lambda(1-v^2)}}} - 1 \right) - 1 \right]. \quad (\text{B.2})$$

One can easily see that the last two formulae arise from (3.16) and (3.17) in the limit of $b \rightarrow 0$. Thus, we can simply set $b = 0$ in (5.18) and obtain

$$E \underset{r \rightarrow 0}{=} \frac{R^2}{\alpha'} \left[-\frac{1}{2\pi\rho^2} \frac{1}{r} + c\rho^2 r \right]. \quad (\text{B.3})$$

This result can be also verified by repeating the calculations of the Section 5 and Appendix A.

The situation with the large distance asymptotics is a little bit more complicated. First, due to the substitution $\lambda \rightarrow 4\lambda$, the limit of $\lambda \rightarrow 2$, which is mapped to the limit of large distances in [9], changes to $\lambda \rightarrow 1/2$. The second issue stems from the fact that the parameter λ contributes to the overall coefficient of the potential. This is also the case in our work: for example, the $e^{2x}U^4(b, 0, x)$ factor in (4.11) is due to λ -containing coefficients. To clarify the second problem it makes sense to reiterate the derivation procedure for the large distance potential once again (this is also described in Ref. [18]).

The main idea goes as follows: since the integrals for non-zero λ diverge in the upper limit, the main contribution to their value comes from the integrands at $v = 1$. Thus, we get

$$r = 2\sqrt{\frac{\lambda}{c}} \int_0^1 \frac{dv}{\sqrt{(1-v)A(\lambda) + (v-1)^2B(\lambda)}}, \quad (\text{B.4})$$

$$E = \frac{R^2}{\pi\alpha'} \sqrt{\frac{c}{\lambda}} e^{2\lambda} \int_0^1 \frac{dv}{\sqrt{(1-v)A(\lambda) + (v-1)^2B(\lambda)}}. \quad (\text{B.5})$$

The new expression under the square root is the result of the series expansions and since the original expressions under the square root were the same for r and E , the expansions above are also the same. Here $A(\lambda)$ and $B(\lambda)$ are some functions, the precise form of which is not important for this discussion. Next, we express the integral from (B.4), substitute it into (B.5) and arrive at

$$E \underset{r \rightarrow \infty}{=} \frac{R^2}{2\pi\alpha'} \frac{c}{\lambda} e^{2\lambda} r. \quad (\text{B.6})$$

Finally, we substitute $\lambda = 1/2$ and obtain the large distance potential,

$$E \underset{r \rightarrow \infty}{=} \frac{R^2}{\pi\alpha'} ecr. \quad (\text{B.7})$$

As an aside we would like to point out that in our reproduction of the results of Ref. [9] we observed that the second function is actually equal to $B(\lambda) = 9\lambda - 2\lambda^2 - 6$ which differs from the corresponding expression in [9]. This difference, however, does not affect the results because the relevant integral is simply canceled in the final formula.

References

- [1] G. S. Bali, *QCD forces and heavy quark bound states*, Phys. Rept. **343** (2001), 1-136, [[hep-ph/0001312](#)]
- [2] E. Eichten, K. Gottfried, T. Kinoshita, K. D. Lane and T. M. Yan, *Charmonium: The Model*, Phys. Rev. D **17** (1978), 3090, [erratum: Phys. Rev. D **21** (1980), 313]

- [3] A. Karch, E. Katz, D. T. Son and M. A. Stephanov, *Linear confinement and AdS/QCD*, Phys. Rev. D **74** (2006), 015005, [[hep-ph/0602229](#)]
- [4] O. Andreev, *$1/q^{*2}$ corrections and gauge/string duality*, Phys. Rev. D **73** (2006), 107901, [[hep-th/0603170](#)]
- [5] J. M. Maldacena, *The Large N limit of superconformal field theories and supergravity*, Adv. Theor. Math. Phys. **2** (1998), 231-252, Int. J. Theor. Phys. **38**, 1113 (1999), [[hep-th/9711200](#)]
- [6] E. Witten, *Anti-de Sitter space and holography*, Adv. Theor. Math. Phys. **2** (1998), 253-291, [[hep-th/9802150](#)]
- [7] S. S. Gubser, I. R. Klebanov and A. M. Polyakov, *Gauge theory correlators from noncritical string theory*, Phys. Lett. B **428** (1998), 105-114, [[hep-th/9802109](#)]
- [8] S. S. Afonin and T. D. Solomko, *Towards a theory of bottom-up holographic models for linear Regge trajectories of light mesons*, Eur. Phys. J. C **82** (2022) no.3, 195, [[2106.01846](#)]
- [9] O. Andreev and V. I. Zakharov, *Heavy-quark potentials and AdS/QCD*, Phys. Rev. D **74** (2006), 025023, [[hep-ph/0604204](#)]
- [10] S. J. Brodsky, G. F. de Teramond, H. G. Dosch and J. Erlich, *Light-Front Holographic QCD and Emerging Confinement*, Phys. Rept. **584** (2015), 1, [[1407.8131](#)]
- [11] S. J. Brodsky, G. F. de Teramond and A. Deur, *Nonperturbative QCD Coupling and its β -function from Light-Front Holography*, Phys. Rev. D **81** (2010), 096010, [[1002.3948](#)]
- [12] A. P. Trawiński, S. D. Glazek, S. J. Brodsky, G. F. de T eramond and H. G. Dosch, *Effective confining potentials for QCD*, Phys. Rev. D **90** (2014) no.7, 074017, [[1403.5651](#)]
- [13] U. Gursoy, E. Kiritsis and F. Nitti, *Exploring improved holographic theories for QCD: Part II*, JHEP **02** (2008), 019, [[0707.1349](#)]
- [14] Y. Chen, D. Li and M. Huang, *The dynamical holographic QCD method for hadron physics and QCD matter*, [[2206.00917](#)]
- [15] S. S. Afonin, *Generalized Soft Wall Model*, Phys. Lett. B **719** (2013), 399-403, [[1210.5210](#)]
- [16] S. S. Afonin, *AdS/QCD models describing a finite number of excited mesons with Regge spectrum*, Phys. Lett. B **675** (2009), 54-58, [[0903.0322](#)]
- [17] J. M. Maldacena, *Wilson loops in large N field theories*, Phys. Rev. Lett. **80** (1998), 4859-4862, [[hep-th/9803002](#)]
- [18] S. Afonin and T. Solomko, *Gluon string breaking and meson spectrum in the holographic Soft Wall model*, Phys. Lett. B **831** (2022), 137185, [[2112.00021](#)]
- [19] J. Sonnenschein, *Stringy confining Wilson loops*, PoS **tmr2000** (2000), 008, [[hep-th/0009146](#)]
- [20] D. V. Bugg, *Four sorts of meson*, Phys. Rept. **397** (2004), 257-358, [[hep-ex/0412045](#)]

- [21] S. S. Afonin, *Towards understanding spectral degeneracies in nonstrange hadrons. Part I. Mesons as hadron strings versus phenomenology*, Mod. Phys. Lett. A **22** (2007), 1359-1372, [[hep-ph/0701089](#)]
- [22] S. J. Brodsky, G. F. de Téramond, H. G. Dosch and C. Lorcé, *Universal Effective Hadron Dynamics from Superconformal Algebra*, Phys. Lett. B **759** (2016), 171-177, [[1604.06746](#)]
- [23] S. S. Afonin, *Towards reconciling the holographic and lattice descriptions of radially excited hadrons*, Eur. Phys. J. C **80** (2020), 723, [[2008.05610](#)]
- [24] Y. Nambu, *Strings, Monopoles and Gauge Fields*, Phys. Rev. D **10** (1974), 4262
- [25] L. Susskind, *Dual symmetric theory of hadrons. 1*, Nuovo Cim. A **69** (1970), 457
- [26] G. Frye, C. W. Lee and L. Susskind, *Dual-symmetric theory of hadrons. 2. baryons*, Nuovo Cim. A **69** (1970), 497
- [27] D. B. Fairlie and H. B. Nielsen, *An analog model for ksv theory*, Nucl. Phys. B **20** (1970), 637
- [28] A. Deur, S. J. Brodsky and G. F. de Teramond, *The QCD Running Coupling*, Nucl. Phys. **90** (2016), 1, [[1604.08082](#)]
- [29] A. L. Kataev and V. S. Molokoedov, *Fourth-order QCD renormalization group quantities in the V scheme and the relation of the β function to the Gell-Mann–Low function in QED*, Phys. Rev. D **92** (2015) no.5, 054008, [[1507.03547](#)]
- [30] S. Godfrey and N. Isgur, *Mesons in a Relativized Quark Model with Chromodynamics*, Phys. Rev. D **32** (1985), 189-231
- [31] P. A. Zyla *et al.* [Particle Data Group], *Review of Particle Physics*, PTEP **2020** (2020) no.8, 083C01
- [32] S. S. Afonin and A. D. Katanaeva, *Glueballs and deconfinement temperature in AdS/QCD*, Phys. Rev. D **98** (2018), 114027, [[1809.07730](#)]